

# SEARCH FOR THE LEPTON-FLAVOUR VIOLATION AT THE LHCb\*

JAKUB MALCZEWSKI

on behalf of the LHCb Collaboration

Institute of Nuclear Physics Polish Academy of Sciences, 31-342 Kraków, Poland

*Received 4 April 2023, accepted 17 April 2023,  
published online 6 September 2023*

This contribution summarizes motivation and experimental methodology of lepton-flavour violation searches, based on the  $B^0 \rightarrow K^{*0} \mu^\pm e^\mp$  and  $B_s^0 \rightarrow \phi \mu^\pm e^\mp$  decays.

DOI:10.5506/APhysPolBSupp.16.7-A31

## 1. Introduction

The completeness of a physics theory can be tested by looking for experimental outcomes that do not follow predictions. Finding such discrepancies would facilitate scientific progress and lead to new discoveries. The Standard Model (SM) is tested in such a manner, but so far, results are consistent with their predictions [1]. A possible new-physics effect that would be in direct disagreement with the SM is the lepton-flavour violation (LFV), which occurs when the lepton number for a given lepton generation is not conserved through a process. An LFV example is the decay involving one electron and one muon, such as:  $B^+ \rightarrow K^+ \mu^- e^+$ ,  $D^+ \rightarrow \pi^+ \mu^- e^+$ . No such or similar process was ever observed.

There is a general agreement on the SM being incomplete, which comes from the lack of answers to the crucial questions about the nature of our Universe. A source of the matter–antimatter asymmetry or the origin of dark matter are still unknown. A discovery of LFV could be the next step to finding some of the answers.

## 2. Lepton-flavour violating processes

In principle, the lepton flavour should be conserved in the SM, but the neutrino oscillations break this rule for neutral leptons. Because of that,

---

\* Presented at the 29<sup>th</sup> Cracow Epiphany Conference on *Physics at the Electron–Ion Collider and Future Facilities*, Cracow, Poland, 16–19 January, 2023.

some LFV decays with charged leptons could occur through the neutrino mixing, as shown in Fig. 1, but the branching fractions of such processes are extremely low [2] and beyond the current experimental sensitivity.

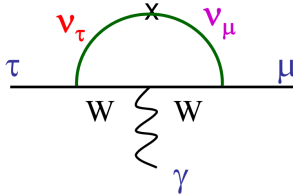


Fig. 1. Example of the LFV process,  $\tau \rightarrow \mu\gamma$  occurring through  $\nu_\tau \rightarrow \nu_\mu$ .

Different extensions of the SM introduce new particles that could mediate LFV decays, for example, leptoquarks, which carry both lepton and baryon numbers [3], or supersymmetric (SUSY) particles [4, 5]. Decay rates predicted by some of the models, in particular for decays of particles containing  $b$  or  $c$  quarks, are within reach of the current high-energy colliders, Belle II and LHCb.

Table 1. Beyond-SM models and their predicted branching ratios of the LFV decays. Symbol  $l$  stands for  $\mu$  or  $e$ .

Models	$\tau \rightarrow \mu\gamma$	$\tau \rightarrow ll\gamma$
SM + $\nu$ mixing [2]	$10^{-54}$ – $10^{-40}$	$10^{-14}$
SUSY + Higgs [4]	$10^{-10}$	$10^{-7}$
SM + Maj $\nu_R$ [6]	$10^{-9}$	$10^{-10}$
Non-universal $Z'$ [7]	$10^{-9}$	$10^{-8}$
mSUGRA + Seesaw [8]	$10^{-8}$ – $10^{-12}$	$10^{-9}$
SUSY SO(10) [5]	$10^{-8}$ – $10^{-10}$	$10^{-10}$
MLFV [9]	$10^{-8}$	
Little Higgs [10]	$10^{-8}$ – $10^{-11}$	$10^{-9}$ – $10^{-11}$

### 3. Lepton reconstruction at the LHCb experiment

The LHCb detector is a single-arm spectrometer that is optimised for measuring decays with  $b$  or  $c$  quarks. Its main advantage is a very precise reconstruction of the primary and secondary vertices. Through years of running, the detector collected  $9 \text{ fb}^{-1}$  of the proton–proton collision data, at the centre-of-mass energies of 7, 8, and 13 TeV. The detector contains multiple specialised sub-detectors. For LFV search purposes, the most important

are the electromagnetic calorimeter and muon stations. The presence of dedicated detectors allows for an efficient muon reconstruction. The electromagnetic calorimeter can register any charged particle and photons, which makes an electron reconstruction much more challenging. Proton–proton interactions at this energy scale create a lot of different particles in a single interaction, which may result in a large combinatorial background for studied processes.

An electron measurement brings an additional complication — the bremsstrahlung radiation. During an interaction with a magnetic field, electrons can emit photons that carry a significant portion of their energy. A similar process for muons is negligible, due to their larger mass. The emitted photon can hit the calorimeter close to the radiating electron hit, which then registers the electron and photon as one particle, or at any point on the intersection of the calorimeter plane and a line tangential to the electron track. Since the tracking detectors do not register neutral particles, matching a proper photon to the electron is not trivial and has to be done during the offline data analysis. This process introduces an additional uncertainty on a measured mass of a decay final state. Sometimes the emitted photon remains undetected or unmatched, which leads to too low reconstructed mass, and in other cases, an incorrectly added photon has too much energy, which makes the measured mass too high. This effect is reflected in the mass distribution of reconstructed particles that have decayed to at least one electron, but it is not present in the case of analogous decays with muons, as shown in Fig. 2.

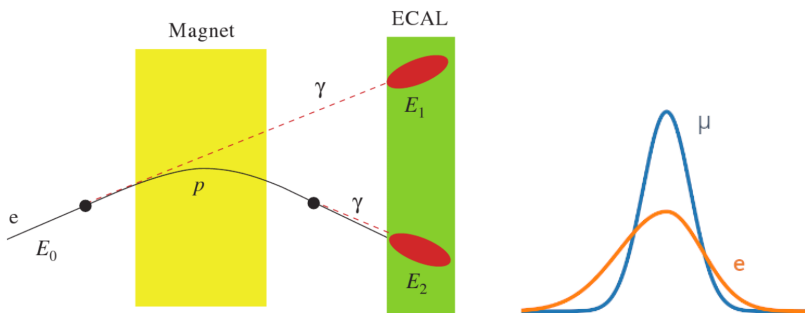


Fig. 2. Illustration of the bremsstrahlung radiation process with two photons emitted by an electron (left) and its typical impact on the final-state mass distribution for decays with electrons at the LHCb, compared to the muon case (right).

#### 4. Search for $B^0 \rightarrow K^{*0} \mu^\pm e^\mp$ and $B_s^0 \rightarrow \phi \mu^\pm e^\mp$ decays

There are many LFV studies performed by the LHCb Collaboration, but most of them follow a similar analysis procedure/method. One of the

recent searches is described in [11]. In this work, authors have analysed the reconstructed events with  $K^{*0}$  decaying to  $K^\pm\pi^\mp$  and  $\phi$  to  $K^\pm K^\mp$  final states. As beyond-SM models can impact the underlying quark-level  $b \rightarrow su^+e^-$  and  $b \rightarrow su^-e^+$  transitions differently, the reconstructed  $B^0$  candidates were divided into two charge categories: the same-sign (as a reference to  $K$  and  $\mu$  charges being the same) for  $B^0 \rightarrow K^+\pi^-\mu^+e^-$  and opposite-sign for  $B^0 \rightarrow K^+\pi^-\mu^-e^+$  decays. Upper limits for these categories are calculated separately. The branching fractions  $\mathcal{B}_{\text{sig}}$  are set in relation to reference decays:  $B^0 \rightarrow J/\psi(\rightarrow \mu^+\mu^-)K^{*0}$  and  $B_s^0 \rightarrow J/\psi(\rightarrow \mu^+\mu^-)\phi$ , with similar final states and well-known branching fractions. The exact formula

$$\mathcal{B}_{\text{sig}} = \frac{\mathcal{B}_{\text{norm}}}{N_{\text{norm}}} \times \frac{\varepsilon_{\text{norm}}}{\varepsilon_{\text{sig}}} \times N_{\text{sig}}$$

includes  $N_{\text{sig}}$  that denotes the measured signal yield and  $N_{\text{norm}}$  that states for the measured normalisation-channel yield under the same selection requirements. The selection efficiencies for the signal and normalisation channels,  $\varepsilon_{\text{sig}}$  and  $\varepsilon_{\text{norm}}$ , are especially important, as they incorporate differences between the signal channel, with the electron and muon, and the normalisation channel with the double muon in the final state. They include the efficiency of every step in the analysis: the particle and decay reconstruction, the trigger selection and the multivariate-analysis selection.

For the final selection, the Boosted Decision Trees (BDT) algorithm is used. It is trained separately for the two-signal decays, with the events from the higher  $B_s^0$  mass sideband as the background proxy and the calibrated simulation for the signal. The BDT selection threshold is chosen based on the Punzi figure of merit [12]:  $\varepsilon_{\text{sig}}/(1.5 + \sqrt{N_{\text{bkg}}})$ , where  $N_{\text{bkg}}$  is the number of expected background events.

After the selection, no signal is observed and the upper limits at 90% (95%) confidence level with a background-only hypothesis are calculated to be

$$\begin{aligned} \mathcal{B}(B^0 \rightarrow K^{*0}\mu^+e^-) &< 5.7 \times 10^{-9} \quad (6.9 \times 10^{-9}) , \\ \mathcal{B}(B^0 \rightarrow K^{*0}\mu^-e^+) &< 6.8 \times 10^{-9} \quad (7.9 \times 10^{-9}) , \\ \mathcal{B}(B^0 \rightarrow K^{*0}\mu^\pm e^\mp) &< 10.1 \times 10^{-9} \quad (11.7 \times 10^{-9}) , \\ \mathcal{B}(B_s^0 \rightarrow K^{*0}\mu^\pm e^\mp) &< 16.0 \times 10^{-9} \quad (19.8 \times 10^{-9}) . \end{aligned}$$

The distributions of the reconstructed  $B_{(s)}^0$  mass, for the two signal decays in the two categories, are presented in Fig. 3 along with the fit results. The main background components included in the fits are the combinatorial and misreconstructed backgrounds from other  $B_{(s)}$  decays, such as semileptonic channels and decays involving excited charm mesons.

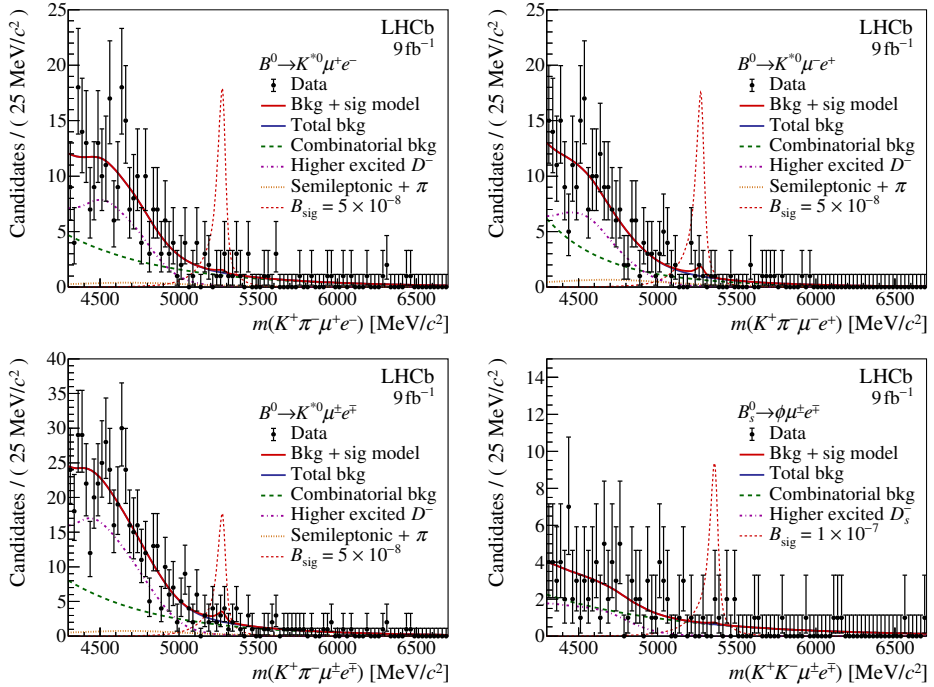


Fig. 3. Mass distributions for (top left)  $B^0 \rightarrow K^{*0} \mu^+ e^-$ , (top right)  $B^0 \rightarrow K^{*0} \mu^- e^+$ , (bottom left)  $B^0 \rightarrow K^{*0} \mu^\pm e^\mp$ , and (bottom right)  $B_s^0 \rightarrow \phi \mu^\pm e^\mp$  candidates. The data are overlaid with the fit results. For illustration, the signal distribution, scaled to a branching fraction of  $5 \times 10^{-8}$  for the  $B^0 \rightarrow K^{*0} \mu^\pm e^\mp$  decays and  $1 \times 10^{-7}$  for  $B_s^0 \rightarrow \phi \mu^\pm e^\mp$ , is also shown.

## 5. Summary

The lepton-flavour violation processes are prime candidates for the beyond-SM effects. Searching for them requires precise measurements of leptons and very good reconstruction technics. Multiple theories that predict LFV could be tested in the near future as the experimental sensitivity improves.

I would like to express my gratitude to the National Science Centre, Poland (NCN), for financial support under contract No. 2018/29/B/ST2/01644. This research was also supported in part by PL-Grid Infrastructure.

## REFERENCES

- [1] H. Gisbert, M. Golz, D.S. Mitzel, *Mod. Phys. Lett. A* **36**, 2130002 (2021).
- [2] T.P. Cheng, L.-F. Li, *Phys. Rev. Lett.* **45**, 1908 (1980).
- [3] B. Diaz, M. Schmaltz, Y.-M. Zhong, *J. High Energy Phys.* **2017**, 097 (2017).
- [4] A. Brignole, A.M. Rossi, *Phys. Lett. B* **566**, 217 (2003).
- [5] T. Fukuyama, A. Ilakovac, T. Kikuchi, *Eur. Phys. J. C* **56**, 125 (2008).
- [6] G. Cvetič, C. Dib, C.S. Kim, J.D. Kim, *Phys. Rev. D* **66**, 034008 (2002).
- [7] C. Yue, Y. Zhang, L. Liu, *Phys. Lett. B* **547**, 252 (2002).
- [8] S. Antusch, E. Arganda, M.J. Herrero, A.M. Teixeira, *J. High Energy Phys.* **2006**, 090 (2006).
- [9] V. Cirigliano, B. Grinstein, *Nucl. Phys. B* **752**, 18 (2006).
- [10] T. Goto, Y. Okada, Y. Yamamoto, *Phys. Rev. D* **83**, 053011 (2011).
- [11] LHCb Collaboration (R. Aaij *et al.*), *J. High Energy Phys.* **2023**, 73 (2023), [arXiv:2207.04005](https://arxiv.org/abs/2207.04005) [hep-ex].
- [12] G. Punzi, [arXiv:physics/0308063](https://arxiv.org/abs/physics/0308063).